27th ABCM International Congress of Mechanical Engineering
December 04-08, 2023, Florianópolis-SC, Brazil

COB-2023-1613
OPTIMIZATION OF A MAGNETOCALORIC AIR CONDITIONER PROTOTYPE

Rogério S. Sucaria
rogerio.sucaria@polo.ufsc.br
Anderson Lorenzoni
anderson.lorenzoni@polo.ufsc.br
Yan Azeredo
yan.azeredo@polo.ufsc.br
Alan T. Nakashima
alan.nakashima@polo.ufsc.br
Guilherme F. Peixer
guilherme.peixer@polo.ufsc.br
Jaime A. Lozano
jaime@polo.ufsc.br
Jader R. Barbosa Jr.
jrb@polo.ufsc.br

POLO – Research Laboratories for Emerging Technologies in Cooling and Thermophysics, Department of Mechanical Engineering, Federal University of Santa Catarina, Florianópolis – SC, Brazil

Abstract. *For the last century vapor compression has been the main technology employed in refrigeration systems, even though it presents drawbacks regarding environmental impacts. To diminish the dependence on this technology and improve energy efficiency, alternative techniques have been explored. Among them, magnetic refrigeration shows some characteristics that stand out, such as the use of solid-state refrigerant, which prevents leakage of harmful substances, and the lack of gases that contribute to global warming. A functional magnetic refrigeration system is made up of four main subsystems: hydraulic management system , heat exchangers, active magnetic regenerator, and a magnetic circuit. Integration of these four subsystems results in the magnetic refrigeration unit. The focus of this work is on the MC-AMR arrangement, which consists of a rotor-stator configuration chosen mainly by its known high cooling capacities. The MC consists of two concentric cylinders that are separated by an air gap where the AMRs are allocated. Through the rotation of the rotor an oscillatory magnetic flux density is applied to each of the individual AMR beds, and with the HMS influence the four steps of the AMR cycle can be performed: magnetization, hot blow, demagnetization, and cold blow. The measured results were then used to obtain the cooling capacities and power consumption for each case tested.*

Keywords: *Magnetic Refrigeration, Active Magnetic Regenerator, Energy Efficiency.*

1. INTRODUCTION

Throughout the decades, refrigeration technology has been a main pillar in the development of modern society. From simple necessities like thermal comfort across all regions in the globe, being able to conserve food for long periods of time, and other functions that can performed with refrigeration, this technology its normally assumed to be present in the daily routine of the majority of the population, assuming its impact and importance. There are many technological alternatives to operate a refrigeration system, being vapor compression the most widespread among them. The technology is a mature solution for refrigeration, being the systems and supply chain developed and optimized over the last century. However, even after a long period of improvements, this alternative has its drawbacks. Among them, the considerable impact this technology has on global warming can be highlighted, especially due to the direct and indirect greenhouse gas emissions associated with its operation.

With these complications, alternatives to the vapor compression system have been explored in the literature. Among them, magnetocaloric technology shows great potential, once it employs a solid-state refrigerant, the Magnetocaloric Material (MCM), and has the potential to operate at high efficiencies, due to the reversible nature of the Magnetocaloric Effect (MCE) (Smith *et al.*, 2012). The MCE is characterized as the thermal response a MCM has when it is submitted to a variable magnetic field, which can be translated into a temperature change, when the process is isentropic, or heat absorption/rejection, when the process is isothermal. One way to obtain such a result from this material for a practical refrigeration application is to assemble the MCM into the so-called active magnetic regenerator (AMR). The most common materials utilized in room temperature magnetic refrigeration are Gadolinium (Gd) and Lanthanum-Iron-Silicon (La-Fe-Si) alloys. The main reason for this is due to their favorable magnetocaloric properties, which include a Curie temperature (the temperature at which the MCE is maximum) close to room temperature and, in the case of La-Fe-Si aloys, which can be tuned through changes in the composition of the materials (Kitanovski *et al.*, 2015; Vieira *et al.*, 2021).

The AMR is the principal component of most modern magnetic refrigeration systems, and operates under a Brayton-like thermomagnetic cycle, which consists of two isentropic processes (magnetization and demagnetization) and two isofield processes (hot and cold blow), all of which with the MCM playing the role of a solid refrigerant and regenerative matrix (Kitanovski *et al.*, 2015; Vieira *et al.*, 2023). To start this cycle, it is necessary to execute an adiabatic magnetization, where a magnetic field is applied to the AMR and the MCM within has it temperature increased through the MCE. This is followed by the next step of the cycle, which is the cold blow, where the work fluid flows from the cold heat exchanger through the regenerator itself, while the magnetic field is kept on the AMR, absorbing heat from the material and rejecting it to the hot recipient. After that, adiabatic demagnetization occurs, which enables the material temperature to decrease, allowing it to reach temperatures below those of the surrounding ambient. Finally, the work fluid from the hot heat exchanger enters the regenerator, rejecting heat to the regenerator itself, lowering its temperature, allowing it to absorb heat on the cold heat exchanger, closing out the cycle. This whole operation results in a complex system that includes multiple areas of study, such as fluid mechanics, heat transfer, material science and magnetism in which several aspects of the design of the AMR and the synchronization between each step of the cycle need to be considered to obtain the best result possible (Vieira *et al.*, 2023).

In recent decades, numerous prototypes have been developed worldwide by both academic and industrial institutions (Greco *et al.*, 2019). Among these institutions, the team at Polo - Research Laboratories for Emerging Technologies in Cooling and Thermophysics, affiliated with the Federal University of Santa Catarina, has been working for over a decade. The group has successfully designed and built various apparatuses, including components evaluation setups (Trevizoli *et al.*, 2016), a rotary prototype (Lozano *et al.*, 2016), a wine cooler (Nakashima *et al.*, 2021; De Sá *et al.*, 2023), and an air conditioning system (Peixer *et al.*, 2023c).

Regarding the air conditioning system, the team performed a system-level optimization process to create a design composed of 16 AMR beds made solely of La-Fe-Si alloys (Nakashima *et al.*, 2022; Peixer *et al.*, 2023b). However, due to limitations in the availability of MCM, only 8 AMR beds were used in the prototype, consisting of a combination of La-Fe-Si and Gd (Peixer *et al.*, 2023c). This setup resulted in the system operating with severe frequency restrictions, achieving a maximum frequency of 0.6 Hz, and a maximum cooling capacity of approximately 490 W, with a maximum temperature span of 16.7°C from the AMR perspective. To improve the performance of the system, the team optimized it by modifying the geometry of the AMR-MC arrangement to accommodate all available MCM mass Peixer *et al.* (2023a). This optimization increased the cooling capacity to 680 W, but decreased the maximum temperature span to 8.7°C. After experimental characterization, a significant degradation of the MCM within the AMR beds was observed, especially in the high Curie temperature La-Fe-Si alloys. Investigating the impact of this degradation on system performance remains an ongoing and complex task which is under execution. In light of the material degradation issue, it is crucial to design a new prototype, considering the degraded La-Fe-Si material.

Therefore, the current work aims to propose a novel configuration for the multilayer arrangement of the AMR, without modifying any aspect or geometry of the remaining components of the system, with a focus on maximizing the utilization of available MCM mass. Additionally, the team plans to conduct an experimental characterization on the redesigned system and assess the proposed modifications in the performance of the prototype.

2. Experimental Apparatus

To carry out the following study, a prototype consisting of a magnetic refrigeration unit (MRU) was developed. This apparatus was designed to operate near room temperature and achieve a maximum cooling capacity of 9000 BTU/h (Peixer *et al.*, 2023b). This system can be separated into four main subsystems, which are the magnetic circuit (MC), the AMRs arrangement, the hydraulic and control systems (HCS), and finally, heat exchangers (HEx). The experimental tests of the prototype were carried out on a calorimeter, which was designed and calibrated specifically for the experimentation of the MRU (Silva *et al.*, 2021). For a complete understanding of the individual components and the overall design of the system, we suggest referring to the publication by Peixer *et al.* (2023c). Furthermore, a visual representation of the MRU (Magnetic Refrigeration Unit) located outside the calorimeter can be found in Fig. 1. For a more detailed visual representation, there is an explanatory video showcasing the MRU and the associated calorimeter accessible at: https://youtu.be/5lVMstvAjgk.

2.1 Magnetic Circuit

The MC is made up of two concentric cylinders, which are separated by a small air gap where the AMRs will be allocated. The interior cylinder is known as the stator, remains static, is made of laminated sheets of electrical steel to reduce losses due to eddy currents, and is responsible for positioning the AMRs and guiding the magnetic flux density.

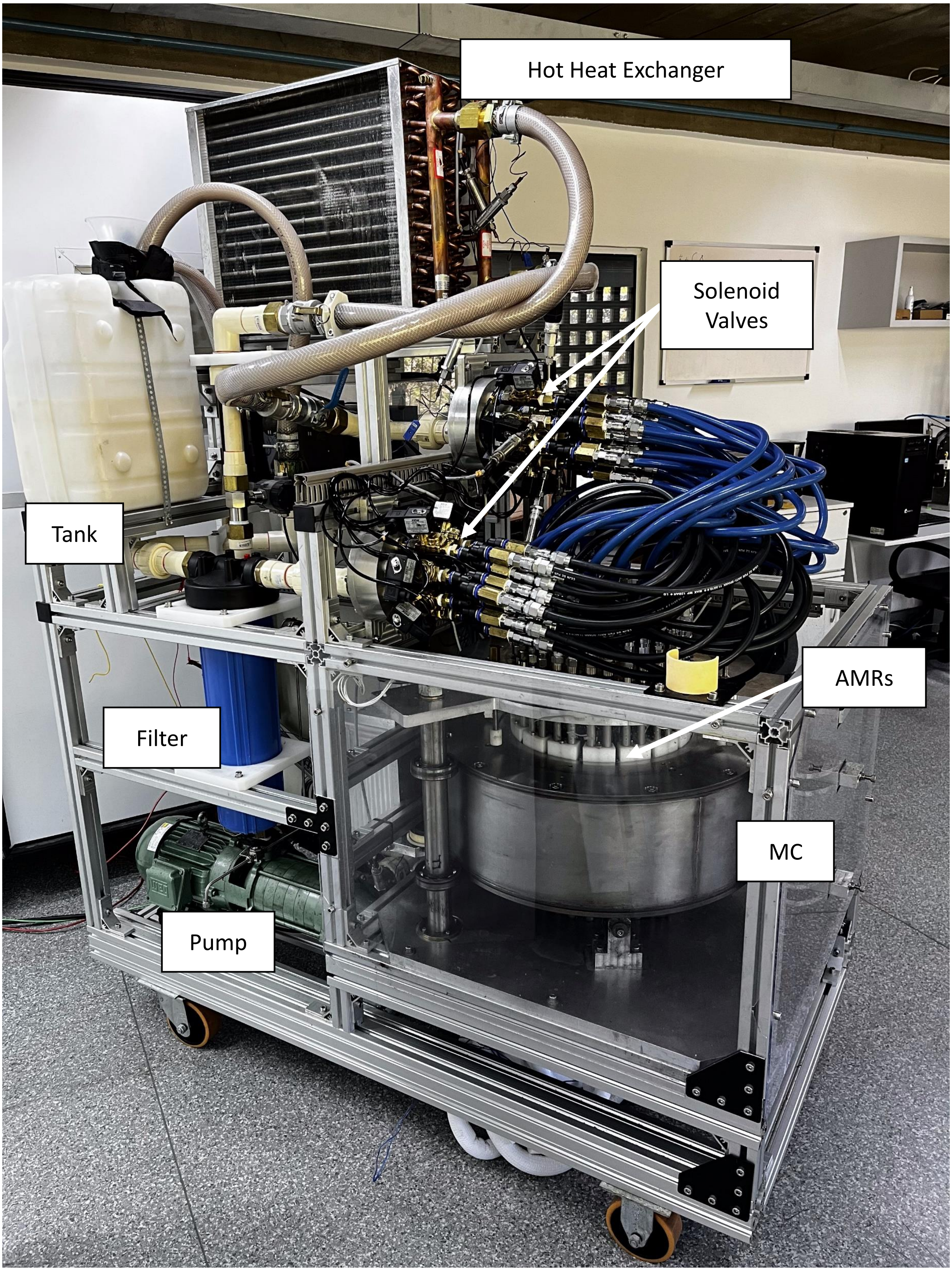

Figure 1. Magnetic Refrigeration Unit

The sheets are stacked around a fixed shaft and tied by two flanges. The outer cylinder,known as the rotor, consists of hard and soft ferromagnetic materials. The soft ferromagnetic region is made up of S235JR laminated sheets, exclusively for manufacturing purposes. For the hard ferromagnetic region, it is composed of 64 epoxy-glued segments of Nd-Fe-B permanent magnets of grades N50M and N42M, with remanence directions designed to optimize the magnetic flux density in the gap between the rotor and the stator (Fortkamp *et al.*, 2023). A servomotor (WEG-SWA-56-4-8-20, driver WEG-SCA06) integrated in a pulley and belt arrangement is the main responsible for rotation of the rotor. A cross-sectional view of a schematic representation of the MC-AMR assembly, where the rotor, stator, shaft, and the original 16 AMR beds is presented in Fig. 2.

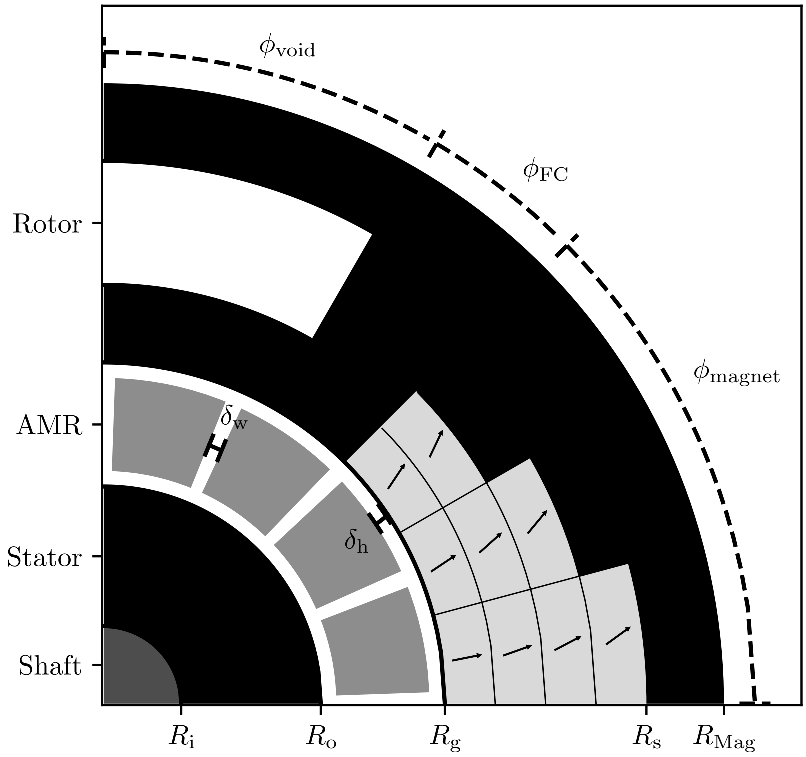

Figure 2. Cross section view of the MC-AMR assembly. Black regions: soft magnetic material; white regions: air; light gray regions: hard magnetic material; gray regions: AMRs; Dark gray region at the bottom left: stator/shaft; arrows: remanence directions Peixer *et al.* (2023b).

The dimensions of R_{Mag}, R_{s}, R_{g}, R_{o} and R_{i} are, respectively, 338, 315, 185, 153, and 34 mm. The length of both the rotor and the stator is 190 mm. The dimensions of δ_{h} are 2 mm and that of δ_{w} is 2.5 mm.

2.2 Active Magnetic Regenerator

The AMRs are attached to the stator in stainless steel casings, which have the shape of a cylindrical shell and are designed to support the cyclical mechanical loads with the minimal thickness possible. In the first version of the system, 8 regenerator beds employed 7.6 kg of La(FeMnSi)$_{13}$H$_z$ alloys (commercialized as *Calorivac-HS2* by Vacuumschmelze GmbH & Co) divided into 10 layers and 2.5 kg of Gd (supplied by the Baotou Research Institute of Rare Earths, China) in a single layer. The second version also used 7.6 kg of La(FeMnSi)$_{13}$H$_z$ into 10 layers and 4 kg of Gd in a single layer. When the AMRs of this last version of the prototype were opened, severe material degradation was observed. Hence, the MCM is being investigated in order to determine which layers still present structural and magnetocaloric properties that are adequate for the operation of a magnetic refrigeration system. It is not known beforehand, but it is expected that there is enough material to operate with 4 or 8 regenerator beds, which will be determined in the following weeks. For the final version of the paper, a complete description of the multilayer composition of the regenerator beds is going to be provided.

2.3 Hydraulic and Control Systems

Hydraulic and control systems have their responsibilities in managing work fluid flow and making sure that the component has the correct amount of mass flow rate and frequency necessary. The work fluid consists of a mixture of water (95%) and anticorrosive fluid (5%). An arrangement of gear pump (Thebe P11/7 5 hp), solenoid valves (ASCO SC8210-112) and check valves (Puma AE-10) is organized as can be seen in the hydraulic diagram presented in Fig. 3, which is necessary to ensure correct oscillatory flow in the AMR (Santos *et al.*, 2021). In Fig. 3, the HMS required for the operation of a magnetic refrigerator with 8 AMR beds is shown. To perform valve actuation, it is controlled by a signal of an encoder coupled to the rotor. As a unit, each pair of regenerators is controlled by a pair of solenoid valves and another pair of check valves. Also, to monitor the coupling between the magnetic profiles and hydraulic a Hall-effects sensor.

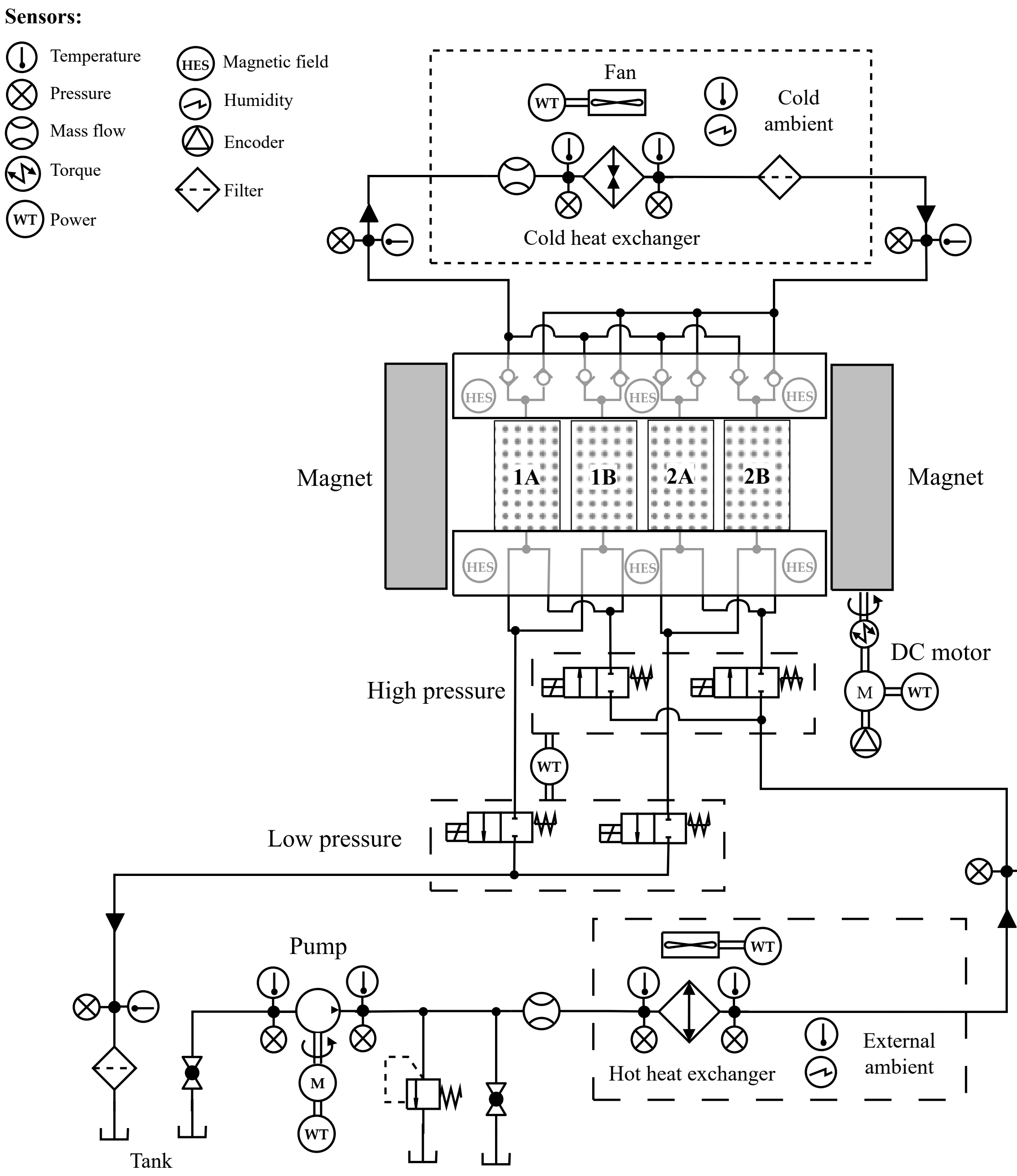

Figure 3. Hydraulic Diagram of the MRU.

To acquire the angular position of the rotor and the magnetic flux is necessary an encoder and 8 Hall-effect sensors, respectively. For the temperature and pressure measurements, it is necessary to obtain them at different positions in the fluid line in the ambient environment. Power transducers are used in pumps, fans, and rotor, which also has a torque meter. Data acquisition and control are then performed with LabVIEW software with National Instruments hardware (cDAQ-9179 and My-Rio 19000).

2.4 Heat Exchangers

The thermal contact between the working fluid and the hot and cold reservoir is the responsibility of the HEx. For their favorable thermal-hydraulic characteristics, fan-supplied multicircuited herringbone-wave tube fin HExs were used (Peixer *et al.*, 2020). These HEx utilized in the MRU have 515 mm height, 550 mm width and 245 mm length, with eight fins per inch, a tube internal diameter of 11.9 mm and wall thickness of 0.4 mm. To force convection, each HEx has an axial fan (Ebm-Papst S4E350-AN19-43).

In terms of calorimeter, it consists of two rooms separated by an insulated wall that reproduces the indoor (cold) and outdoor (hot) ambient. The MRU is positioned in the former, whereas the CHEx is positioned in the latter. The walls are insulated with polyisocyanurate which has a thermal conductivity between 0.02 $\mathrm{Wm^{-1}K^{-1}}$ and 0.03 $\mathrm{Wm^{-1}K^{-1}}$. To separate the chambers, an internal wall with the thickness of 150 mm is used, while the other walls have a thickness of 70 mm. Temperature, pressure, power consumption, humidity, and condensed water mass are measured in the calorimeter (Silva *et al.*, 2021).

3. Performance Metrics

An evaluation of the performance of the system as a whole is carried out by evaluating the coefficient of performance, COP, the cooling capacity, $\dot{Q}_\mathrm{c}$, and the second law efficiency, η, from both the point of view of the system and the AMR. Regarding the AMR standpoint, its parameters are usually compared with other magnetocaloric refrigerators, while the parameters used for the system perspective are better suited to compare with the convectional mechanical compression system. The cooling capacity of the system can be calculated by:

$$\dot{Q}_\mathrm{C} = \dot{m}_\mathrm{f} c_\mathrm{p} \Delta T_\mathrm{c,reg} \tag{1}$$

where c_p is the specific heat of the working fluid, $\dot{m}_\mathrm{f}$ is the mass flow rate of the system and the $\Delta T\mathrm{c,reg}$ is the is the temperature difference between the fluid temperature entering the cold end of the AMR during the cold blow and leaving the cold end of the AMR during the hot blow, which are measured in the low- and high-pressure cold manifolds, respectively.

The regenerator temperature spans ΔT_reg, usually employed for magnetic refrigeration systems, is defined as:

$$\Delta T_\mathrm{reg} = T_\mathrm{HE} - T_\mathrm{CE} \tag{2}$$

where T_HE is the fluid temperature in the outlet manifold at the hot side; T_CE is measured at the corresponding spot at the cold end.

The Coefficient of Performance from the system COP_sys standpoints can be calculated by:

$$COP_\mathrm{sys} = \frac{\dot{Q}_\mathrm{c}}{\dot{W}_\mathrm{pp} + \dot{W}_\mathrm{rt} + \dot{W}_\mathrm{CHEx} + \dot{W}_\mathrm{HHEx} + \dot{W}_\mathrm{sv}} \tag{3}$$

where in Eq. (3) $\dot{W}_\mathrm{pp}$ is the pump power consumption, $\dot{W}_\mathrm{CHEx}$ and $\dot{W}_\mathrm{HHEx}$ are the power consumption of the fans in Cold and Hot Heat Exchangers, respectively, $\dot{W}_\mathrm{rt}$ is the power consumption to drive the rotor of the magnetic circuit, $\dot{W}_\mathrm{sv}$ is the power consumption necessary for the actuation of the solenoid valves, which are all measured by power transducers.

4. RESULTS

The thermodynamic performance of the prototype was evaluated under several operating conditions, in order to map the results and determine the most favorable values to operate at. For that, three mass flow rates (400, 600, and 800 kg $\mathrm{h^{-1}}$) and two frequencies (0.5 and 1 Hz) were evaluated. It is worth mentioning that deviations in the mass flow rate achieved by some of the tests were encountered due to instabilities during the experiment and mass flow rate measurements. Additionally, blow fractions (BF), which is defined as the period in which a blow occurs compared to the entire period of the AMR cycle, of 35 and 40% were also evaluated, resulting in a total of 12 experiments, where the design space was mapped seeking to encounter the optimal conditions for the operation of the system. For the experiments carried out in the present analysis, the temperature of the hot environment was kept at 18ºC to operate in a region that would be suitable for the Curie temperatures of the magnetocaloric materials. The results of the cooling capacity for the different experiments are shown in Fig. 4.

Several remarks on the operation of magnetic refrigeration systems can be taken by evaluating Fig. 4. First, the best results, that is, the largest cooling capacities were, in general, achieved in higher frequencies. The exceptions occurred at 400 kg $\mathrm{h^{-1}}$, where the results for all conditions reached similar values. That is determined by a trade-off between the effectiveness of the porous medium, viscous dissipation of the fluid flow, and the displaced mass of fluid, which is also responsible for the peaks encountered at 600 L $\mathrm{h^{-1}}$. Hence, as the frequency increases, there are more cycles done per second, and as the mass flow rate increases, there is more displaced fluid available for cooling the cold environment, but also at a higher temperature as the effectiveness of the regenerator decreases and the heat dissipate due to viscous losses rises.

Additionally, the effect of the blow fraction has opposing effects at 0.5 and 1 Hz. At lower frequencies, by reducing the blow fraction, there is an increase in cooling capacity, whereas for higher frequencies there is a decrease. That is explained since at the lower frequency there is a larger period, and as the blow fraction increases not only does the fluid displaced increase, reducing more viscous losses and effectiveness loss, but also the mean magnetic field applied over the cycle decreases. At higher frequencies, since there is less time for the fluid to flow, the extended period provided by an increase in the blow fraction is advantageous for the operation of the system, surpassing the effects of the loss in the regenerator effectiveness, reduction in the mean magnetic field, and increase in the viscous dissipation.

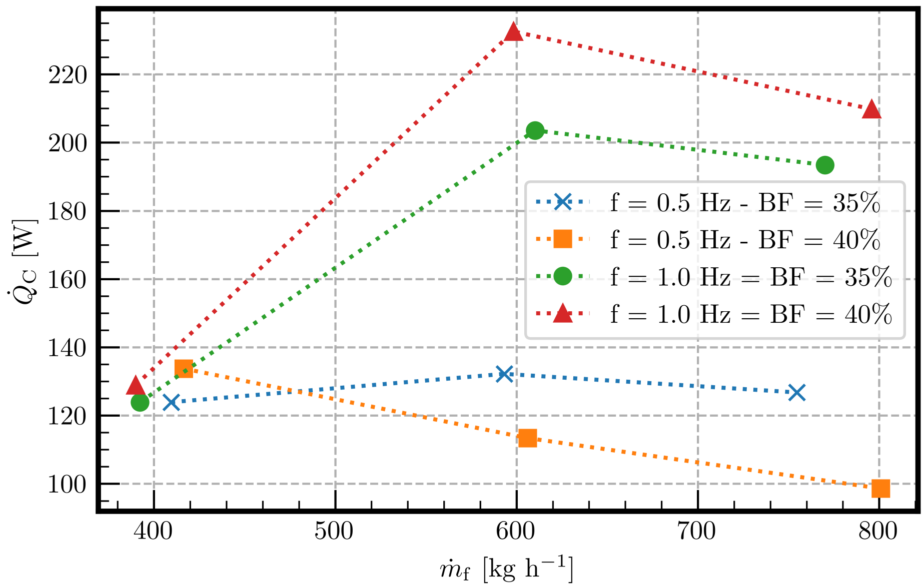

Figure 4. Effect of the operating conditions on the cooling capacity

Following, the results for the temperature span for the different experiments are depicted in Fig. 5. In general, it can be observed that an increase in the mass flow rate results in an increase in the regenerator temperature span, as depicted in the Figure. The only exception is the experiment carried out at 750 kg h^{-1}, 0.5 Hz and with a blow fraction of 35%. The dynamics of the temperature span follow a complex and intricate series of trade-offs, which are dependent not only on the effect of the operating conditions of the active magnetic regenerator but also on their influence on the effectiveness of the heat exchangers and on their coupling with the hot and cold heat reservoirs.

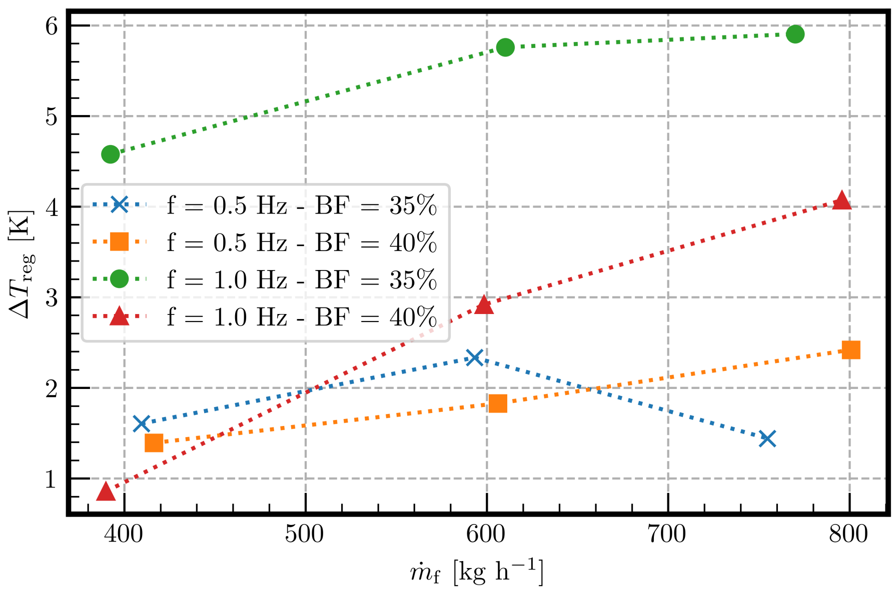

Figure 5. Effect of the operating conditions on the temperature span

For that, in general, as the mass flow rate increases, there is an increase in the effectiveness of the heat exchanger given by a rise in the ratio of the heat capacity rate of the fluid streams, and other factors that cannot be independently quantifiable with the current instrumentation such as fluid mixing, flow maldistribution, losses to void volumes and heat gain to the ambient. Moreover, it is clear that the best conditions were achieved at higher frequencies, according to the results obtained for the cooling capacity, being the best conditions achieved with a blow fraction of 35%, a result of the active magnetic regenerator being under the application of a magnetic flux intensity with higher magnitudes in this condition. At 0.5% those behavior was not observed, which is attributed to the complex dynamics involved in the operation of the system.

Lastly, the results for the COP for the different experiments are shown in Fig. 6. The power consumption of the system is expected to increase along with the frequency, mass flow rate, and blow fraction of the prototype. However, the cooling capacity also rises along with some of those variables; hence, a trade-off behavior is expected to occur in the COP of the system. According to Fig. 6, the best results of the system were achieved at 1 Hz, 600 kg h^{-1} and with a blow fraction of 40%.

At 1 Hz, an optimum point is achieved at 600 kg h^{-1}, while operating at 40% of blow fraction always resulted in better values for the COP. That is due to the behavior depicted in Fig. 4, where the exact same trend happens. Hence, even though there is an increase in the power consumption of the system, the enhancement of the cooling capacity dictates the best operating points in terms of the COP. Moreover, at 0.5 Hz the increase in the cooling capacity is not sufficient to overcome the increase in power consumption, and COP has a decreasing behavior with respect to the mass flow rate for the whole space mapped in the present evaluation.

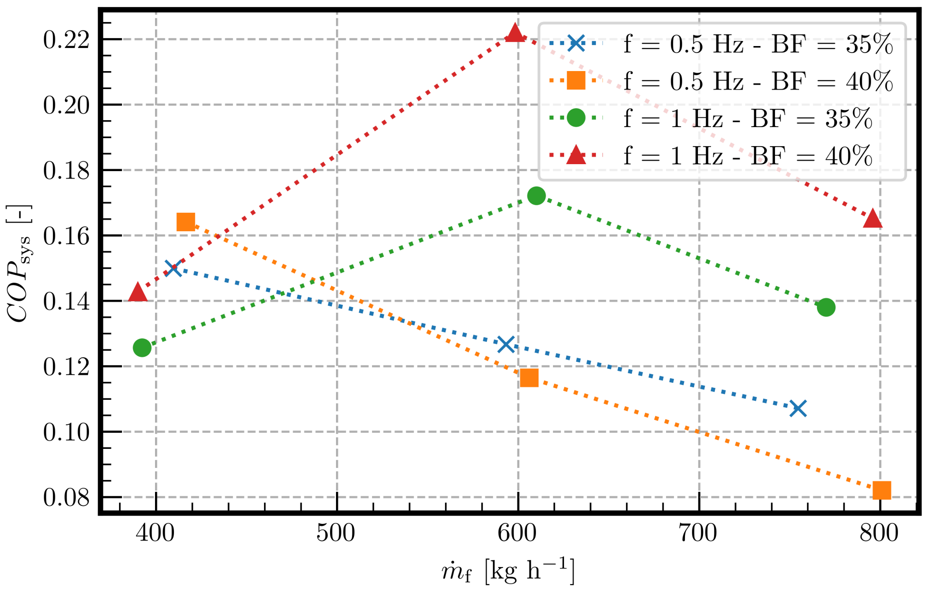

Figure 6. Effect of the operating conditions on the COP

The results presented in Figs. 4- 6 demonstrate that the results achieved by the prototype are still comparable to those achieved by Peixer *et al.* (2023c) and Peixer *et al.* (2023a) when comparing by taking into account the total mass of magnetocaloric materials. However, the influence of the multilayer arrangement and the lack of first-order magnetocaloric materials prevents the system from achieving higher temperature spans. Hence, the availability and reliability of the magnetocaloric material is a critical issue for the prototype to achieve the expected result and also for the development of magnetocaloric refrigeration technology.

5. CONCLUSIONS

Magnetocaloric refrigeration is a promising not-in-kind cooling technology that has the potential for the decarbonization of the refrigeration industry by providing a solution without volatile fluids that can operate with higher energy efficiencies. However, several challenges still hinder the application of those systems. This work presented an optimization of a large-scale prototype which was carried out given the degradation of part of the magnetocaloric material in previous versions.

In this updated version, only 4 active magnetic regenerators were employed, rather than the original 16 that were designed in the original version of the prototype. An experimental assessment of the performance of the system was carried out, where the mass flow rate, frequency, and blow fraction were varied. The results demonstrated that the optimal operating point regarding the cooling capacity and COP was at 600 L h^{-1}, 1 Hz and 40% of the blow fraction and for the temperature span at 800 L h^{-1}, 1 Hz and 35% of the blow fraction. The results achieved are comparable to the ones of the previous versions on a magnetocaloric mass basis but still fall short for practical applications.

6. ACKNOWLEDGEMENTS

Financial support from CNPq, FAPESC, CAPES, CODEMGE, and the EMBRAPII Unit Polo/UFSC is duly acknowledged.

7. REFERENCES

De Sá, N.M., Nakashima, A.T.D., Pagnan, E., Lorenzoni, A., Luz, G.M., Hoffmann, G., Peixer, G.F., Lozano, J.A. and Barbosa, J.R., 2023. "PoloMag Project: Designing a compact magnetocaloric wine cooler". in Proceedings. doi: 10.18462/iir.icr.2023.0840.

Fortkamp, F.P., Nakashima, A.T., dos Santos, V.M., Lozano, J.A. and Barbosa, J.R., 2023. "Computationally-efficient optimization of the remanence angles of permanent magnet circuits for magnetic refrigeration". *Journal of Magnetism and Magnetic Materials*, Vol. 569, p. 170429. ISSN 0304-8853.

Greco, A., Aprea, C., Maiorino, A. and Masselli, C., 2019. "A review of the state of the art of solid-state caloric cooling processes at room-temperature before 2019". *International Journal of Refrigeration*, Vol. 106, pp. 66–88. ISSN 0140-7007. doi:https://doi.org/10.1016/j.ijrefrig.2019.06.034.

Kitanovski, A., Tusek, J., Tomc, U., Plaznik, U., Ozbolt, M. and Poredos, A., 2015. *Magnetocaloric Energy Conversion from Theory to Applications*. Springer.

Lozano, J.A., Capovilla, M.S., Trevizoli, P.V., Engelbrecht, K., Bahl, C.R. and Barbosa Jr., J.R., 2016. "Development of a novel rotary magnetic refrigerator". *International Journal of Refrigeration*, Vol. 68, pp. 187 – 197.

Nakashima, A.T., Fortkamp, F.P., de Sá, N.M., dos Santos, V.M., Hoffmann, G., Peixer, G.F., Dutra, S.L., Ribeiro, M.C., Lozano, J.A. and Barbosa Jr., J.R., 2021. "A magnetic wine cooler prototype". *International Journal of Refrigeration*, Vol. 122, pp. 110–121. ISSN 0140-7007. doi:https://doi.org/10.1016/j.ijrefrig.2020.11.015.

Nakashima, A., Peixer, G., Lozano, J. and Barbosa, J., 2022. "A lumped-element magnetic refrigerator model". *Applied Thermal Engineering*, Vol. 204, p. 117918. ISSN 1359-4311.

Peixer, G.F., Dutra, S.L., Calomeno, R.S., de Sá, N.M., Lang, G.B., Lozano, J.A. and Barbosa Jr., J.R., 2020. "Influence of heat exchanger design on the thermal performance of a domestic wine cooler driven by a magnetic refrigeration system". *Anais da Academia Brasileira de Ciências,*, Vol. Accepted for publication.

Peixer, G.F., Lorenzoni, A.M., Azeredo, Y.C., Silva, P.M., Silva, M.C.R., Hoffmann, G., dos Santos, D., Dutra, S.L., do Rosário, G.M., Teza, H., Pagnan, E., Sucaria, R.S., Doring, A., Rosa, M.A.A., Faria, P., Vieira, B.P., Nakashima, A.T., Wendhausen, P.A.P., Teixeira, C.S., Lozano, J.A. and Barbosa Jr., J.R., 2023a. "Thermodynamic Performance Evaluation of a Magnetocaloric Air Conditioner Prototype". in Proceedings. doi:10.18462/iir.icr.2023.0895.

Peixer, G.F., Nakashima, A.T., Lozano, J.A. and Barbosa, J.R., 2023b. "System-level multi-objective optimization of a magnetic air conditioner through coupling of artificial neural networks and genetic algorithms". *Applied Thermal Engineering*, Vol. 227, p. 120368. ISSN 1359-4311.

Peixer, G.F., Silva, M.C., Lorenzoni, A., Hoffmann, G., dos Santos, D., do Rosário, G.M., Pagnan, E., Teza, H.F., Silva, P.M., Dutra, S.L., Ribeiro, M.C., Rosa, M.A., Döring, A., Vieira, B.P., Nakashima, A.T., Wendhausen, P.A., Teixeira, C.S., Lozano, J.A. and Barbosa, J.R., 2023c. "A magnetocaloric air-conditioning system prototype". *International Journal of Refrigeration*. ISSN 0140-7007. doi:https://doi.org/10.1016/j.ijrefrig.2023.03.014.

Santos, D.D., Dutra, S.L., Ribeiro, M.C., Lorenzoni, A.M., Rosário, G.M.D., Silva, M.C.R., Hoffmann, G., Peixer, G.F., Lozano, J.A. and Barbosa Jr., J.R., 2021. "Designing a hydraulic management system for a large-scale magnetic refrigerator". In *Proceedings in Nineth IIR International Conference on Caloric Cooling, Thermag IX*. Maryland, USA.

Silva, M.C.R., Rosário, G.S., Dutra, S.L., Capovilla, M., Lima, R., Lorenzoni, A., dos Santos, D., Hoffmann, G., Peixer, G.F., Lozano, J.A. and Barbosa Jr., J.R., 2021. "Development and characterization of a calibrated calorimeter to evaluate air conditioning systems." In *Proceedings of the 26th ABCM International Congress of Mechanical Engineering*. Florianópolis, Brazil. doi:10.26678/ABCM.COBEM2021.COB2021-1992.

Smith, A., Bahl, C.R., Bjørk, R., Engelbrecht, K., Nielsen, K.K. and Pryds, N., 2012. "Materials challenges for high performance magnetocaloric refrigeration devices". *Advanced Energy Materials*, Vol. 2, pp. 1288–1318.

Trevizoli, P.V., Nakashima, A.T., Peixer, G.F. and Barbosa, J.R., 2016. "Performance evaluation of an active magnetic regenerator for cooling applications – part i: Experimental analysis and thermodynamic performance". *International Journal of Refrigeration*, Vol. 72, pp. 192–205. ISSN 0140-7007. doi:https://doi.org/10.1016/j.ijrefrig.2016.07.009.

Vieira, B.P., Bez, H.N., dos Santos, D., Lozano, J.A. and Jr, J.R.B., 2023. "Interrelationship between flow profiles and the magnetic waveform and their influence on the performance of first-order active magnetic regenerators". *Applied Thermal Engineering*, Vol. 219.

Vieira, B.P., Bez, H.N., Kuepferling, M., Rosa, M.A., Schafer, D., Cid, C.C.P., Vieyra, H.A., Basso, V., Lozano, J.A.

and Jr, J.R.B., 2021. "Magnetocaloric properties of spheroidal la(fe,mn,si)13h granules and their performance in epoxy-bonded active magnetic regenerators". *Applied Thermal Engineering*, Vol. 183.

8. RESPONSIBILITY NOTICE

The authors are solely responsible for the printed material included in this paper.